

# Detector and physics simulation using heavy ion collisions at NICA-SPD

R. Pandey<sup>1,a)</sup>

<sup>1</sup>Larsen & Toubro Limited, Faridabad-121003, Haryana, India.

<sup>a)</sup>rishav160999@gmail.com

## ACKNOWLEDGEMENT

The author expresses his gratitude to Dr. Igor Denisenko from the Joint Institute for Nuclear Research, Dubna, Russia, for his invaluable support and guidance throughout this research.

## Abstract

The space-time picture of hadron formation in high-energy collisions with nuclear targets is still poorly known. The tests of hadron formation was suggested for the first stage of SPD running. They will require measuring charged pion and proton spectra with the precision better than 10%. A research has been carried out to check feasibility of such studies at SPD. In this work,  $^{12}C - ^{12}C$  and  $^{40}Ca - ^{40}Ca$  heavy ion collisions at center of mass energy of 11 GeV/nucleon were simulated using the SMASH event generator. Firstly, the generator-level events were studied. The distribution of track multiplicities and momentum distributions of different types of charged particles were obtained. Secondly, the generated events passed through the full reconstruction using the SpdRoot framework. At this stage, particles were identified using  $dE/dx$  measurement and time-of-flight information. It allowed us to estimate charge track multiplicities in the tracking system and purities of charge particles spectra. The results on multiplicity are important to estimate occupancies in the tracking system, while the results on the pion and proton momentum spectra show that particle identification should be acceptable for validation of hadron formation models. This is the first study of moderate ion collisions for the SPD Experiment.

**Keywords:** Hadron formation effects, Heavy ion collision, SMASH, NICA-SPD, Rapidity, Charged track multiplicity, Particle physics event generator.

# 1 INTRODUCTION

The SPD detector is primarily optimized to study spin dependent gluon structure of proton and deuteron using open charm production, charmonia production, and prompt photons. At the same time, its physics program includes studies of various aspects of QCD. The work is devoted to studies of hadron formation in nuclear collisions proposed in Ref. [1].

Hadrons produced in hadron collisions emerge in the form of prehadrons, which interact with nucleons with reduced strength. This suppression is poorly known and is described in model dependent way. This suppression results in different spectra of final particles as is illustrated in Fig.1 for rapidity distributions (in a similar way it affects the  $p_T$  spectrum). Naturally, these spectra can be used to study hadron formation effects. The required precision of such measurements is 10%.

The aim of this work is to evaluate feasibility of such measurements with MC simulation. Here, ion collisions of  $^{12}\text{C} - ^{12}\text{C}$  and  $^{40}\text{Ca} - ^{40}\text{Ca}$  at  $\sqrt{s} = 11\text{A GeV}$  were generated using the SMASH (Simulating Many Accelerated Strongly-interacting Hadrons) event generator. Afterwards, the full simulation and reconstruction was performed using the SpdRoot framework.

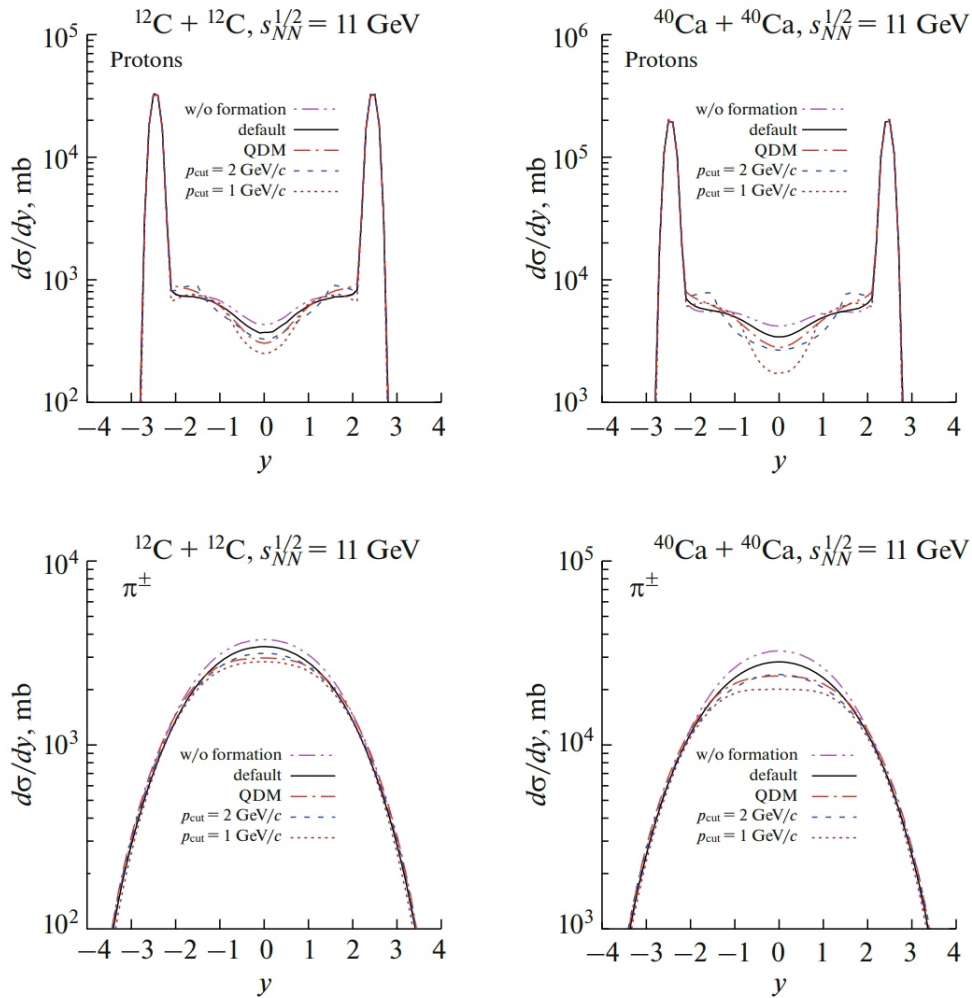


Figure 1: Rapidity spectra of protons and charged pions in  $^{12}\text{C} - ^{12}\text{C}$  and  $^{40}\text{Ca} - ^{40}\text{Ca}$  collisions.

## 2 NICA FACILITY

The NICA (Nuclotron based Ion Collider facility) collider at Joint Institute for Nuclear Research in Dubna is being built to provide beams for two experiments. The first experiment, MPD (Multi Purpose Detector), will study properties of dense baryonic matter (matter present at extreme high density in QCD phase diagram) like Quark Gluon Plasma. The second experiment, SPD (Spin Physics Detector), is devoted to study of spin related phenomena and QCD. Once the NICA collider will be operational, scientists will be able to create a special state of matter in laboratory which existed for very short interval of time ( $\sim 20\mu$  sec) just after the big bang. This special state is called as QGP (Quark Gluon Plasma) and it filled the entire universe shortly after the big bang.

The main parts of NICA facility consists of two independent injector complex (injector for light ions, and injector for heavy ions-KRION 6T), Light Ion Linear Accelerator (LU20) for accelerating light ions like protons ( $H^+$ ), deuterons, and  $\alpha$ -particles upto 5 MeV of K.E, then Heavy Ion Linear Accelerator (HILAC) to accelerate heavy ions upto Au to a maximum K.E of 3.2 MeV/n, then a Super Conducting (SC) Booster Synchrotron to create ultra high vacuum and to provide complete stripping of heavy ions, then a SC Heavy Ion Synchrotron Nuclotron to accelerate both light and heavy ions to required beam energy. The accelerated beams will collide at two different locations where MPD detector and SPD detector are being built. The schematic view of NICA complex is shown in Fig.2.

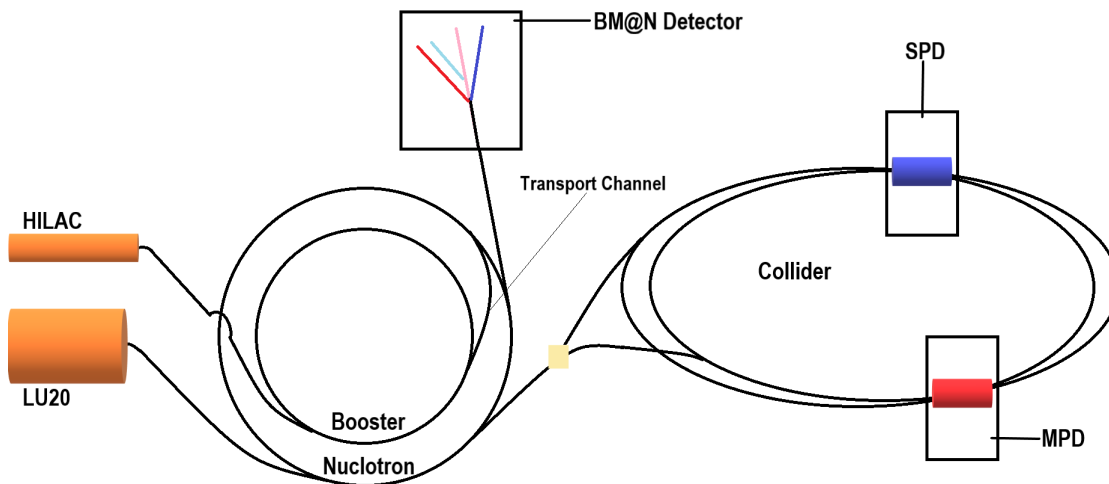
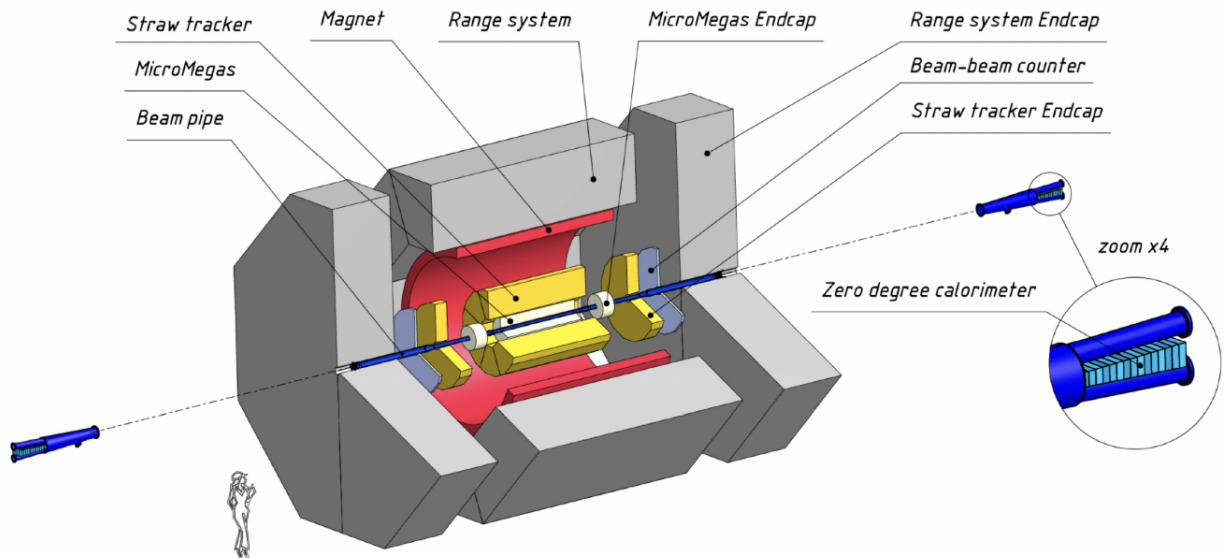


Figure 2: Schematic view of NICA complex.

## 3 SPD DETECTOR

The Spin Physics Detector [2,3] is a  $4\pi$  universal detector optimized to study spin-related phenomena via open charm, charmonia, and prompt photons in the collisions of polarized p-p or d-d beams with  $\sqrt{s_{NN}}$  up to 27 GeV. However, at first stage of NICA-SPD, the expected collision energy will be from 3.4 up to 10 GeV, and later on after first upgrade, it is expected to reach upto 27 GeV. The general layout depicting isometric projection of SPD setup is shown in Fig.3. The main parts involved in advanced tracking and particle identification capabilities have been shown. (i) The beam pipe passes through the center of the detector, carries the accelerated beams of ions. (ii) The MicroMegas detector is to improve the momentum resolution and tracking efficiency of the tracking system. (iii) The Straw Tracker (ST) detector is for the reconstruction of the primary and

secondary particle tracks and for determination of their momenta. (iv) The Time Of Flight (TOF) detector, is a part of Particle Identification (PID) system, and is used for identification of particles like  $\pi$ ,  $k$ , and  $p$  with long trajectories. (v) The magnet system shown by red color provides  $1T$  of magnetic field along the beam axis. This setup is limited to first stage of SPD operation, and will be considered only for the identification of stable charged particles. Neutral particles, like  $n^0$ , photons will be detected at later stages. The main parts of SPD first stage have been explained in detail below. There is a possibility to have TOF system for the first stage studies.



**Figure 3:** Layout of the SPD setup proposed for first stage at NICA-SPD.

### 3.1 CENTRAL TRACKER

The innermost detector of SPD consists of a MicroMegas-based Central Tracker (MCT). Its purpose is to identify the primary vertex coordinate and to improve momentum resolution and tracking efficiency. It is based on MicroMegas (Micro Mesh Gaseous Structure) technology and detects charged particle by amplifying the charges produced due to ionization of the gas molecules present in detector volume. When an ionizing particle track passes through detector volume, it ionizes the gas molecules and creates few hundreds of  $e^-$ -ion pair. Electrons are accelerated opposite to the direction of applied electric field of  $600 \text{ V/cm}$  in ionization gap, while ions are attracted towards cathode. When the  $e^-$  crosses micromesh, it faces intense electric field ( $> 30 \text{ KV/cm}$ ) and gains enough energy to ionize other gas molecules in its path. During this process an avalanche of  $e^-$ -ion pair is produced ( $1e^-$  produces  $10^4 e^-$ -ion pairs) which is significant to create an electronic signal which is read out by readout electrodes.

### 3.2 STRAW TRACKER

ST is mainly for the reconstruction of primary and secondary particle tracks and measuring their momenta, but also participates in identification of  $\pi$ ,  $K$ , and  $p$  on via energy deposit ( $dE/dx$ ) measurements. It consists of two major parts - barrel (covers radius from  $270$  to  $850 \text{ mm}$ ) and two end-caps. The barrel is divided into 8 modules enclosed in a carbon fiber capsule. Each module has 30 double layers of straw tubes (dia  $1\text{cm}$ ) which runs parallel (long straw tubes) and perpendicular

(short straw tubes) to the beam axis and contains 1500 and 6000 parallel and perpendicular straw tubes respectively. Straw tubes are made of polyethylene terephthalate and outer surface is coated with very thin layer of Cu and Au. Carbon capsule is meant to protect the outer surface of these tubes from humidity. One side and two opposite ends of capsule are provided with small holes where end plugs are fixed. FEE are connected to these end plugs to read the detector signal. Any particle which passes through the long straws will send detector signal to both opposite ends while a particle passing through short straw will send detector signal to any one side of capsule where FEE is attached. Thus, long straws will be read from two opposite ends while short straws will be read from one side. The end-caps of ST are divided into 3 modules and each module has 4 hexadecimal cameras (U, V, X, Y) to record the four coordinates of any physical quantity like four-momentum. The FEE to be used can be similar to the one used at NA64 experiment (for the search of dark matter), or DUNE experiment (to detect and study properties of neutrino).

### 3.3 TIME OF FLIGHT DETECTOR

TOF detector is the part of PID system. Similar to ST, the TOF provides identification of  $\pi$ , k, and p by measuring their flight time. The energy loss data registered by ST can be used together with the data from TOF for correct identification of particle tracks. The TOF distinguishes charged particles (mainly  $\pi$  and k) in the momentum range up to 1.5 GeV. The major parts of TOF comprises of a barrel and two end-caps. For the first stage of NICA-SPD, two different designs of TOF has been suggested. First one is TOF based on multigap timing Resistive Plate Chambers (mRPC), which will consist 220 rectangular plate chambers (160 for the barrel and 30 each for end-caps). Second one is based on Plastic Scintillator Tiles and will comprise 10.1K small scintillator tiles (7.4K for barrel and 1.4K for each end-caps). Scintillator has a property of emitting light in visible region when an ionizing radiation passes through it. So, in this design when a particle passes through TOF, scintillated photons are produced which are detected by four Si Photo Multipliers (SiPMs) present at each sensor board attached at two extreme ends of scintillator tile.

## 4 EVENT GENERATION

$^{12}C - ^{12}C$  and  $^{40}Ca - ^{40}Ca$  heavy ion collisions at  $\sqrt{s} = 11$  AGeV with maximum impact parameter set to 8 fm for C-C and 11 fm for Ca-Ca were simulated using SMASH. The fermi motion was assumed to be “frozen” and 100K events were generated for each heavy ion collision. The SMASH input file for C-C collision is shown below.

```
***** SMASH INPUT *****
```

```
config.yaml file for C-C collision.
```

```
Logging:
```

```
  default: INFO
```

```
General:
```

```
  Modus:          Collider
```

```
  Time_Step_Mode: Fixed
```

```
  Delta_Time:     0.1
```

```
  End_Time:       200.0
```

```
  Randomseed:    -1
```

```
  Nevents:       100000
```

```

Output:
  Output_Interval: 10.0
  Particles:
    Format:      ["Oscar2013"]
Modi:
  Collider:
    Projectile:
      Particles: {2212: 6, 2112: 6} #C-12
    Target:
      Particles: {2212: 6, 2112: 6} #C-12
  Sqrtsnn: 11.0
  Impact:
    Sample: "quadratic"
    Range: [0.0, 8.0]
  Fermi_Motion: "frozen"

```

\*\*\*\*\*

Multiplicity of generated charged particles for  $C - C$  and  $Ca - Ca$  collisions are shown in Fig. 4. The peaks at 12 for  $^{12}C+^{12}C$  collisions and at 40 for  $^{40}Ca+^{40}Ca$  collisions correspond to events where no interaction occurred. The rapidity distributions are shown in Fig. 5. The spectra obtained from SMASH output show qualitative agreement with the ones in Fig. 1. Peaks for protons correspond to particles moving close to the initial beam direction. Moreover, fractions of different particle types can be estimated. It can be seen that for  $|y| < 2$  (i.e. within the acceptance of the detector) charge particles are dominated by pions. Apart from  $p^\pm, \pi^\pm$ , &  $K^\pm$ , marginal numbers of sigmas, cascades, and omegas were also generated. The PID efficiency depends on the particle momentum. The momentum spectra for protons, pions, and kaons are shown in Fig. 6 in the midrapidity region ( $|y| < 0.5$  for which theoretical predictions has been given) Most of the pions have momentum below 0.8 GeV and protons - below 1 GeV. It means that types of these particles should be well resolved by  $dE/dx$  measurements. When studying pion or proton spectra, there is high probability of kaon/pion misidentification, but fraction of such events is strongly suppressed by small initial kaon numbers.

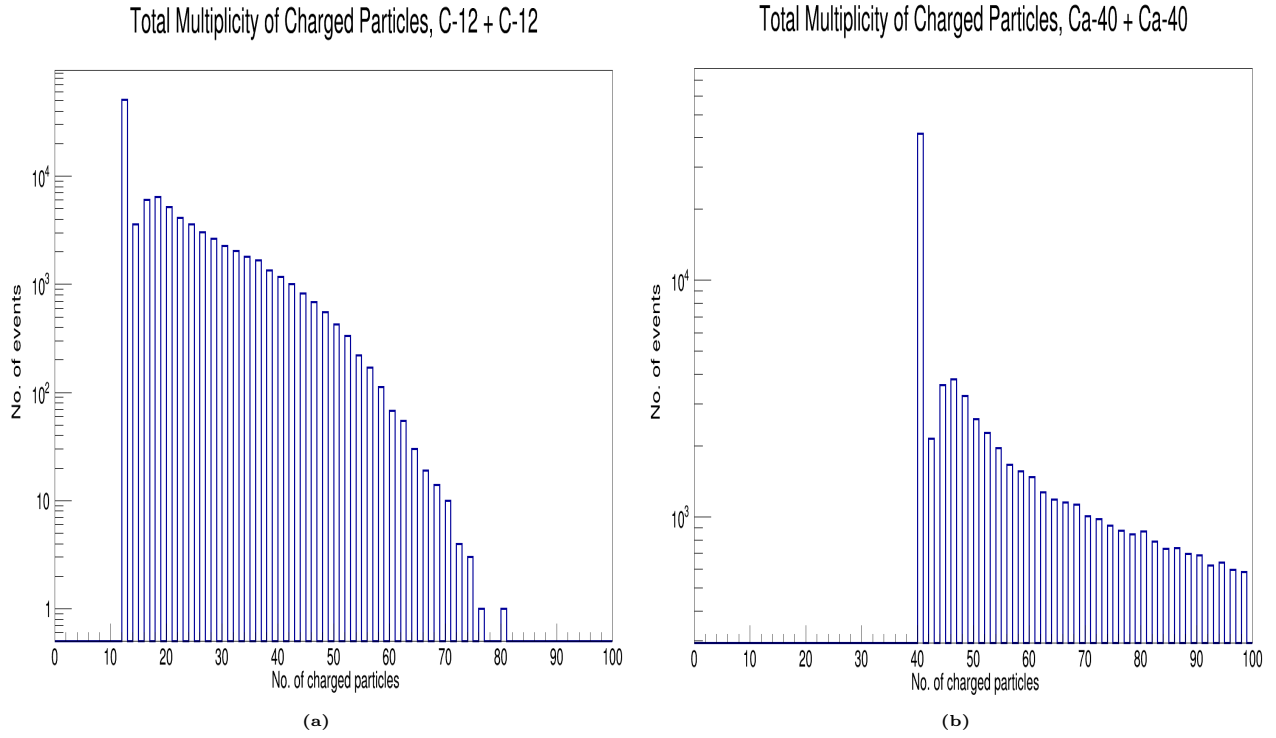


**Figure 4:** Generator-level multiplicity of charged particles for  $^{12}\text{C} - ^{12}\text{C}$  collision (a) and  $^{40}\text{Ca} - ^{40}\text{Ca}$  collisions (b).

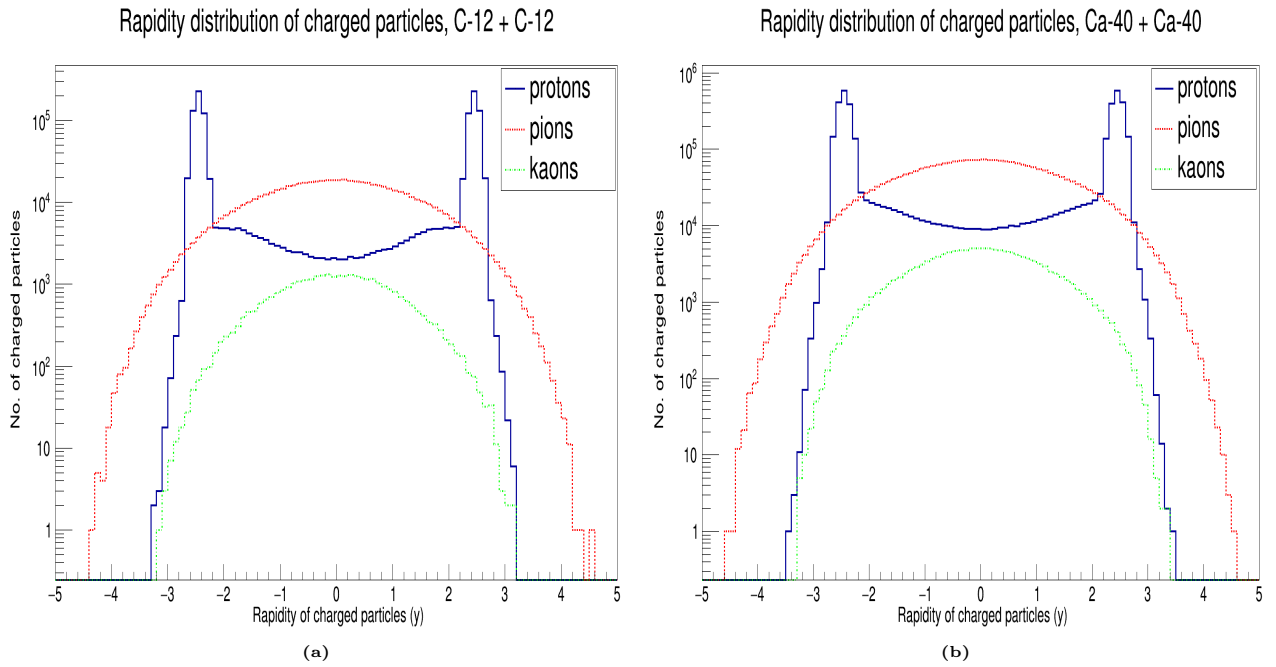
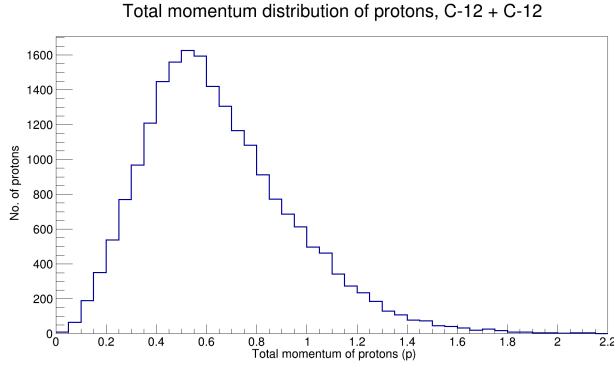
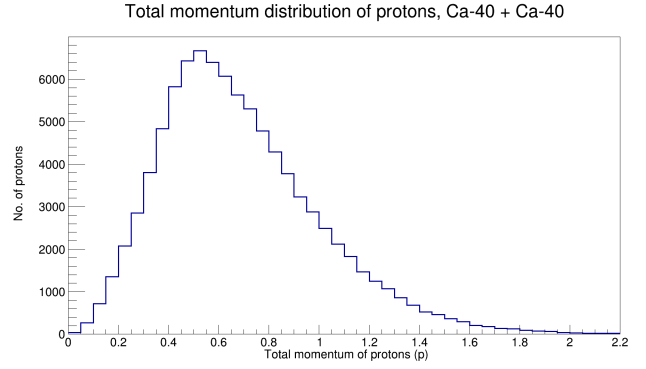


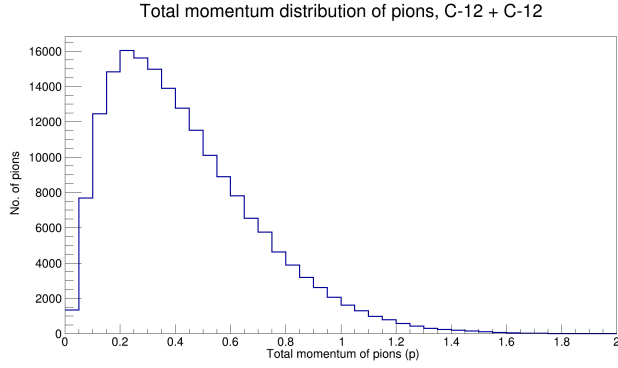
**Figure 5:** Rapidity distribution of charged particles in  $^{12}\text{C} - ^{12}\text{C}$  (a) and  $^{40}\text{Ca} - ^{40}\text{Ca}$  (b) collision.



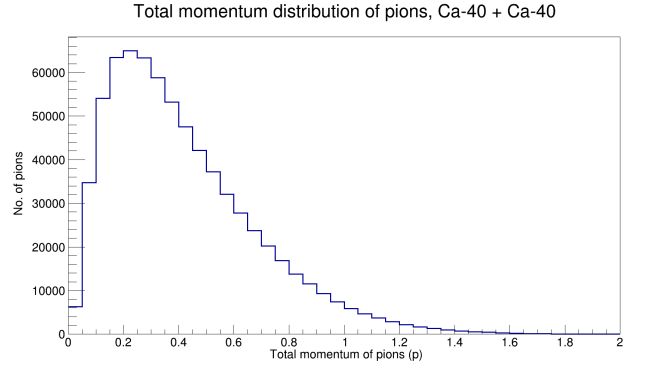
(a) p distribution of  $p^\pm$  in  $^{12}\text{C} - ^{12}\text{C}$  collision.



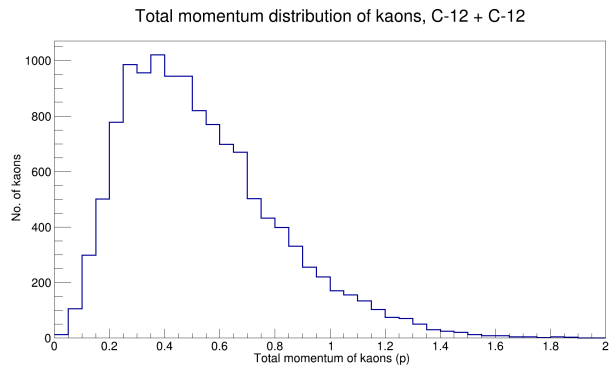
(b) p distribution of  $p^\pm$  in  $^{40}\text{Ca} - ^{40}\text{Ca}$  collision.



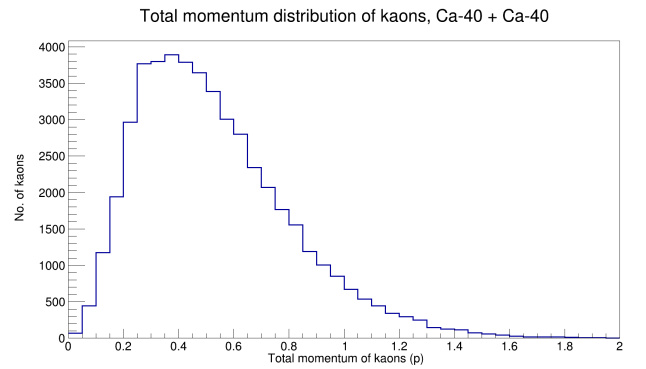
(c) p distribution of  $\pi^\pm$  in  $^{12}\text{C} - ^{12}\text{C}$  collision.



(d) p distribution of  $\pi^\pm$  in  $^{40}\text{Ca} - ^{40}\text{Ca}$  collision.



(e) p distribution of  $k^\pm$  in  $^{12}\text{C} - ^{12}\text{C}$  collision.



(f) p distribution of  $k^\pm$  in  $^{40}\text{Ca} - ^{40}\text{Ca}$  collision.

**Figure 6:** Total momentum distribution of protons, pions, and kaons at generator level in  $^{12}\text{C} - ^{12}\text{C}$  and  $^{40}\text{Ca} - ^{40}\text{Ca}$  collision.



## 5 DETECTOR SIMULATION AND EVENT RECONSTRUCTION

The detector simulation and reconstruction was performed with the SpdRoot framework. To read SMASH generated events the SpdRoot code was modified and additional C++ class was added. During the simulation stage the particles were transported through the detector geometrical model using Geant4. At the reconstruction stage, Geant4 tracks and vertices were reconstructed and particle identification with  $dE/dx$  and time of flight measurements was performed. For the PID three hypotheses were considered: pion, kaon, and proton. The reconstructed ionization energy losses and “measured” time of flight were used to construct conditional probabilities (e.g.  $p(t|pid)$ , where  $t$  is the measured time and  $pid$  is a particle type hypothesis). Out of 100K events generated by SMASH, first 1K events were considered for detector simulation due to slow data processing in SpdRoot.

## 6 ANALYSIS

A physical analysis was performed using C++ codes and ROOT library based on SpdRoot output. All tracks reconstructed in the detector with measured momentum were accepted. For the particle type the one that gives the largest conditional probability is adopted. Multiplicity, as well as kinematic distributions for pions, kaons, and protons are studied. For particle momentum spectra there are no notable differences between  $C - C$  and for  $Ca - Ca$  collisions, so only the first ones will be considered.

### 6.1 CHARGED TRACK MULTIPLICITY

The SPD detector set-up is optimized for  $p - p$  and  $d - d$  collisions. Thus, knowing charged track multiplicities for ion collisions is important to estimate CT and ST occupancies and feasibility of such studies. Fig. 7 shows the total multiplicity of charged particles reconstructed by the tracking system in  $^{12}C - ^{12}C$  and  $^{40}Ca - ^{40}Ca$  collisions. The numbers of reconstructed tracks are much lower compared to generator-level studies. It is because the geometry of the tracking system is such that, tracks with polar angle,  $\theta < 10^\circ$  or  $> 170^\circ$  do not hit the tracker and passes along the beam pipe itself, so such tracks are ignored. Also, there were events without nuclei interactions which resulted in no track reconstruction. So, to avoid a large peak at zero due to mentioned reasons, the X-axis count starts from 1.

### 6.2 PION MOMENTUM SPECTRUM ( $^{12}C - ^{12}C$ )

The spectra of particles identified as pions separately by ionization losses and by TOF are shown in Fig. 8 separately. The spectra show resemblance with the generator plot of pion momentum distribution. Based on MC-truth information background from misidentification other charged particles ( $K^\pm, p^\pm, e^\pm, \& \mu^\pm$ ) is studied. The obtained distribution for “pions identified as pions” only slightly deviates from distribution of all selected pion candidates. The estimated relative contamination of the pion spectra is shown in Fig. 9. It can be seen that purity above 90% can be obtained up to 1.2 GeV using either  $dE/dx$  or TOF measurements.

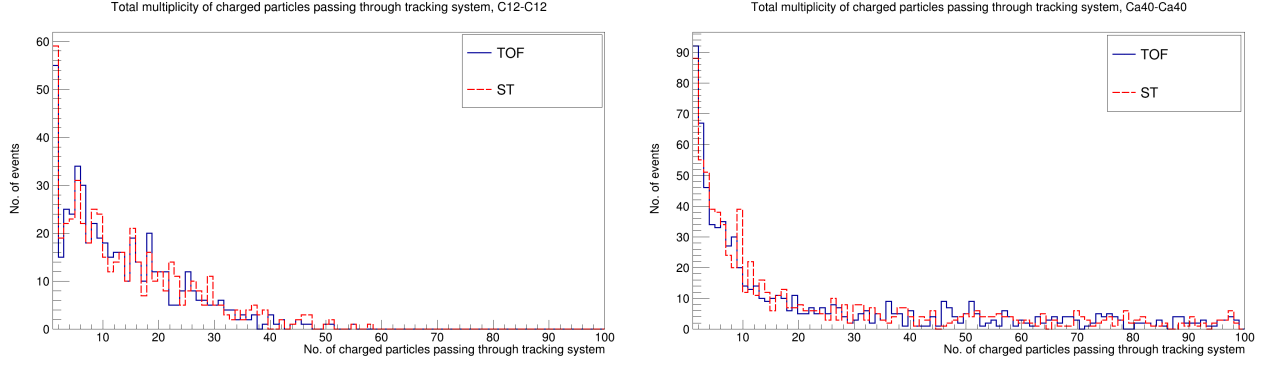
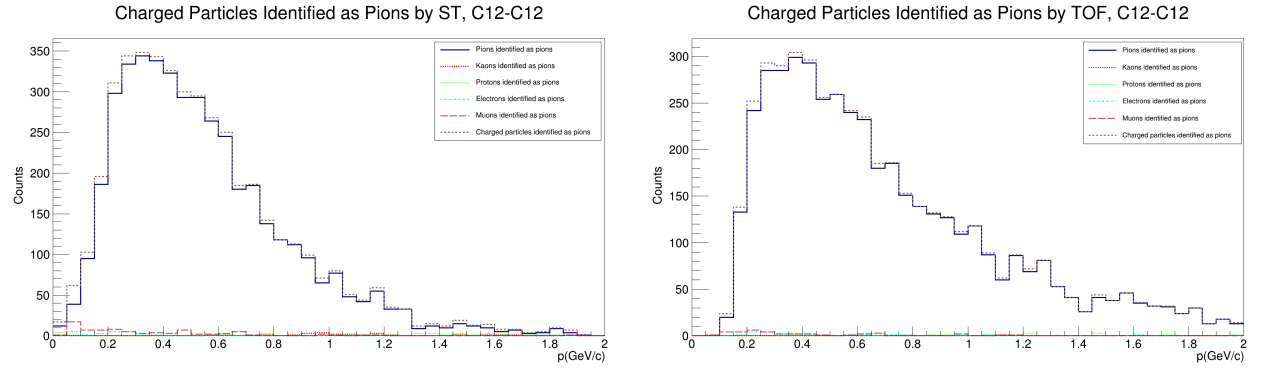


**Figure 7:** Charged track multiplicity reconstructed by in  $^{12}\text{C} - ^{12}\text{C}$  (left),  $^{40}\text{Ca} - ^{40}\text{Ca}$  (right) collisions (shown by red) and number of particles for which TOF information is available (shown by blue).



(a) Total momentum distribution of reconstructed charged particles identified as  $\pi^\pm$  by ionization losses.

(b) Total momentum distribution of reconstructed charged particles identified as  $\pi^\pm$  by TOF.

**Figure 8:** Total momentum distribution of reconstructed  $\pi^\pm$  candidates in  $^{12}\text{C} - ^{12}\text{C}$  collision (Detector level).

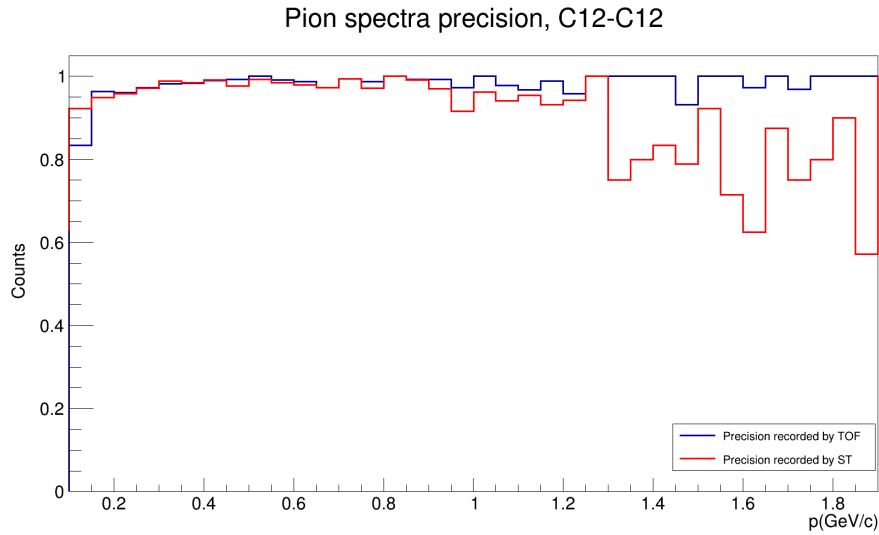


**Figure 9:** Purity of the selected pion candidates as a function of their momentum.

### 6.3 KAON MOMENTUM SPECTRUM ( $^{12}C - ^{12}C$ )

The kaon momentum spectrum was explicitly mentioned among observables to study hadron formation effects in nuclei. Nevertheless, kaon production may be interesting for the reasons. The obtained spectra of kaon candidates is shown in Fig. 10 separately for ionization losses and TOF. First of all, the shown data lack statistics. Secondly, it can be seen that there is a huge contamination from misidentified pions. This is explained by very small fraction of generated kaons and the fact that probability to select misidentified particle is proportional to their number. The relative fraction of correctly identified kaons is shown in Fig. 11.

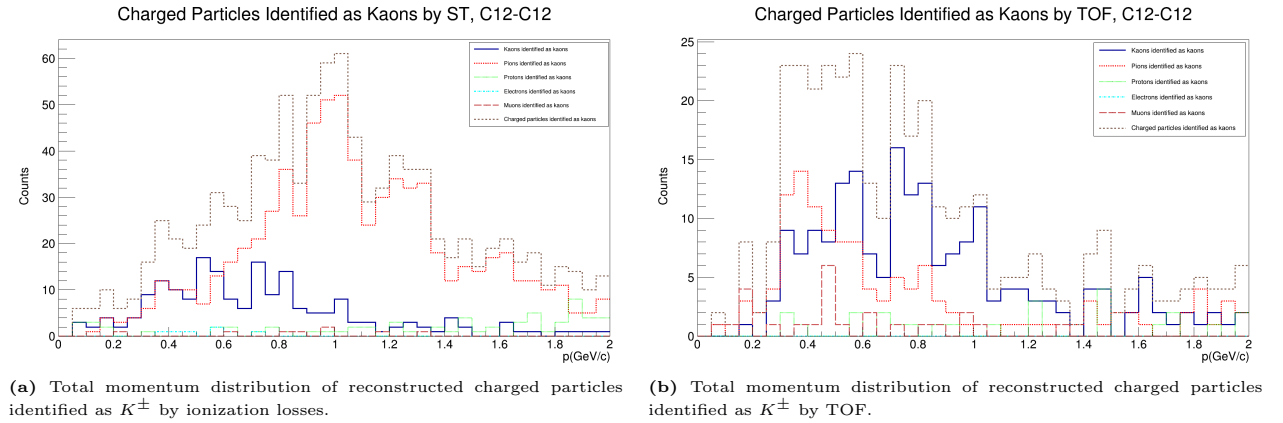


**Figure 10:** Total momentum distribution of reconstructed  $K^\pm$  candidates in  $^{12}C - ^{12}C$  collision (Detector level).

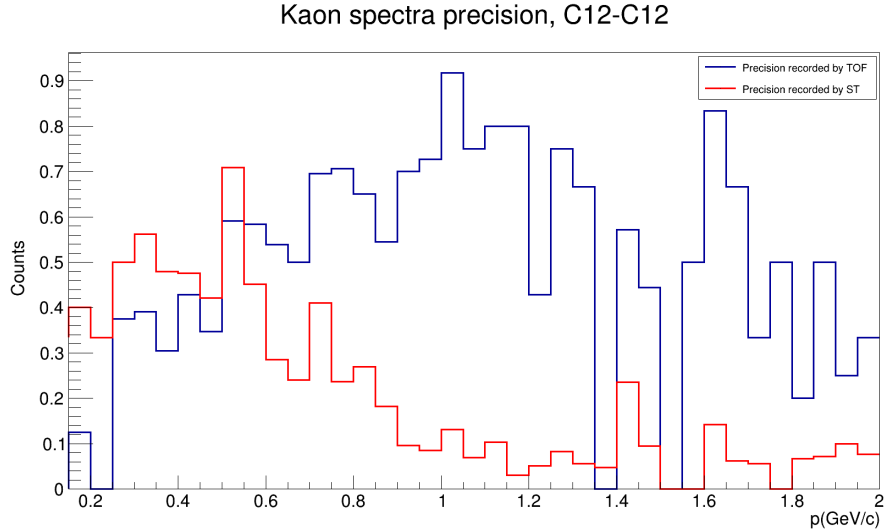


**Figure 11:** Purity of the selected kaon candidates as a function of their momentum.

## 6.4 PROTON MOMENTUM SPECTRUM ( $^{12}C - ^{12}C$ )

Finally, proton momentum spectra have been considered. In this study protons and antiprotons were considered together, but the fraction of produced antiprotons is negligible. The proton candidate distributions and the contributions from misidentification are shown in Fig. 12. The purity of the selected samples is shown in Fig. 13. It can be seen  $dE/dx$  measurements alone will not allow precise determination of proton spectrum. The reasonably good results can be expected only in case of combined identification by ionization losses and TOF system.

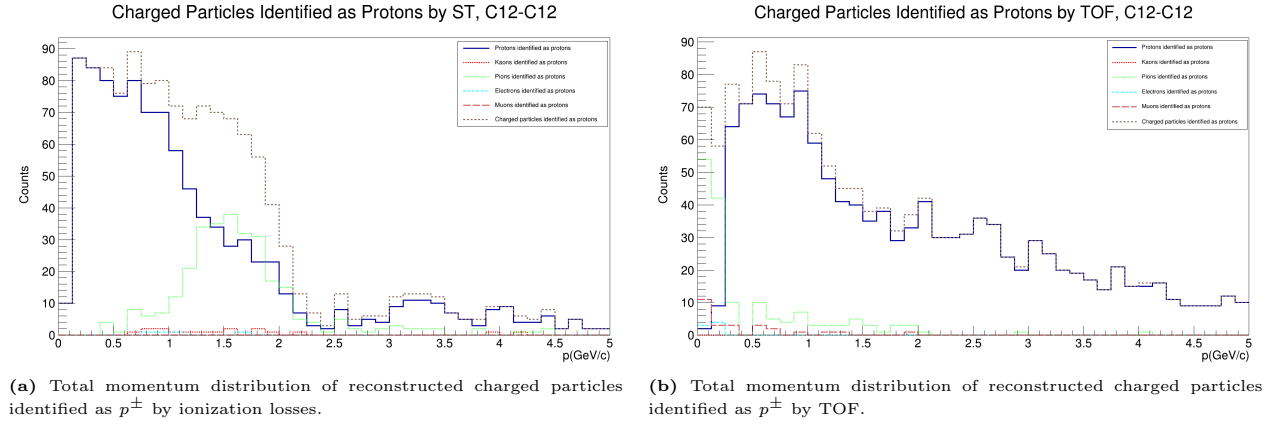


**Figure 12:** Total momentum distribution of reconstructed  $p^\pm$  candidates in  $^{12}C - ^{12}C$  collision (Detector level).

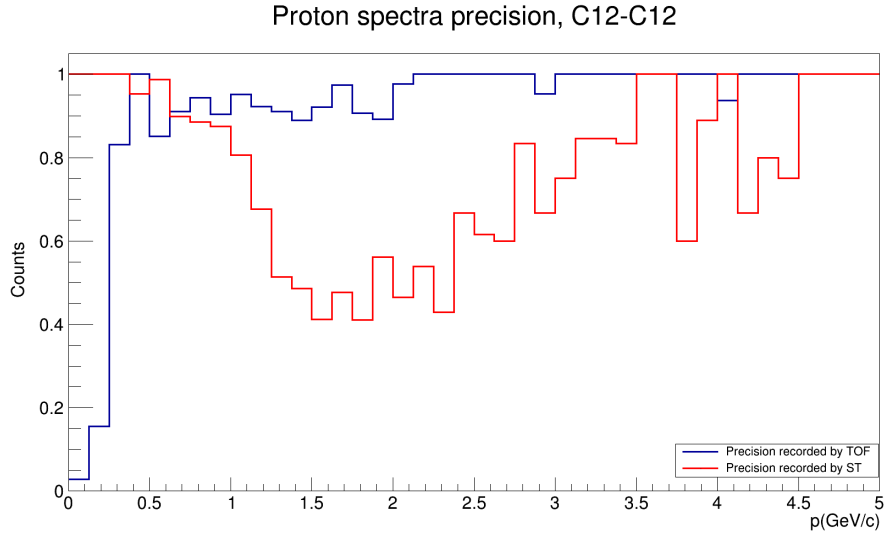


**Figure 13:** Purity of the selected proton candidates as a function of their momentum.

## 7 SUMMARY

The goal of this work was to check the feasibility of hadron formation effects studies at the first stage of SPD operation. For this purpose an analysis of  $^{12}C - ^{12}C$  and  $^{40}Ca - ^{40}Ca$  collisions were performed at the generator level and then the full event reconstruction was done at detector level. The multiplicity distributions indicate that occupancies of tracking detectors should be checked. Part of the events with high number of charged tracks may not be fully reconstructed. Particle identification with ionization losses and TOF was considered separately (for future  $dE/dx$  only or their combination can be expected). The purity of the measured charged pion distribution for both types of ion collisions using  $dE/dx$  only is rather good and meets mentioned before requirements. In case of combination of information from ionization losses and time of flight system purity of proton distribution may be improved.

## References

- [1] V. V. Abramov, A. Aleshko, V. A. Baskov, E. Boos, V. Bunichev, O. D. Dalkarov, R. El-Kholy, A. Galoyan, A. V. Guskov and V. T. Kim, *et al.* Phys. Part. Nucl. **52** (2021) no.6, 1044-1119 doi:10.1134/S1063779621060022 [arXiv:2102.08477 [hep-ph]].
- [2] V. M. Abazov *et al.* [SPD proto], [arXiv:2102.00442 [hep-ex]].
- [3] SPD TDR [unpublished].